The definite version is published in Proc. IEEE Vehicular Technology Conf. (VTC spring), Singapore, 2024.

# Calculating the Traffic Density in LPWANs with Finite Retransmissions

Udo Schilcher[1], Stavros Toumpis[2], Siddhartha S. Borkotoky[3], Jorge F. Schmidt[4], and Christian Bettstetter[1]
[1] University of Klagenfurt, NES, Austria [2]Athens University of Economics and Business, Greece
[3]Indian Institute of Technology Bhubaneswar, India [4]Digital Factory Vorarlberg, Dornbirn, Austria
udo.schilcher@aau.at, toumpis@aueb.gr

***Abstract*—For randomly distributed nodes sending packets to a central gateway using slotted Aloha with a constrained number of retransmissions over a wireless fading channel, we take an iterative approach to compute the total traffic density of packet transmissions and collision-induced retransmissions as a function of the node-gateway distance. From this, we compute the outage probability, throughput, and energy consumption. This method can be used to analyze and dimension Low-Power Wide-Area Networks (LPWANs). Applying it in LoRa illustrates design tradeoffs concerning outage probability, spreading factors, energy consumption, and cell size. It notably shows that permitting more retransmissions helps the nodes near the gateway but hurts distant ones.**

***Index Terms*—IoT, LoRa, LPWAN, massive IoT, performance evaluation, stochastic geometry, wireless network, vehicular IoT.**

## I. Introduction

In this work we propose and analyze a stochastic geometry model of a single-cell system with nodes sending packets to a central gateway using slotted Aloha, where unreceived packets can be retransmitted with a limited number of tries. The nodes are distributed according to a Poisson point process (PPP) and transmissions are successful iff their Signal to Interference and Noise Ratio (SINR) exceeds a threshold. We develop a method for computing the density of the traffic created (including the retransmissions) as a function of the distance $d$ to the gateway. From this, we compute the outage probability, throughput, and energy consumption. Our work is motivated by Low-Power Wide-Area Networks (LPWANs), where slotted Aloha is a common choice, either for packets or for preambles that reserve transmission slots. We apply our methodology to LoRa [1], [2] and arrive at some results revealing fundamental tradeoffs. However, the methodology is general enough to have wider applicability to other LPWAN technologies, such as SigFox [3] and NB-IoT [4], in both fixed and mobile (e.g., [5]) settings.

Our work has a novel aspect in the context of LPWANs: it captures the fact that the levels of interference experienced by a node at different slots are correlated. Very frequently, as an approximation these levels are assumed to be *independent*, as discussed in Section II. This assumption is motivated by settings where *(i)* nodes are *highly* mobile, so that the topology changes drastically from slot to slot, or *(ii)* retransmission attempts are sufficiently separated in time. This assumption leads to drastic simplifications of the analysis, but can also lead to a significant overestimation of the network's performance if it does not hold in reality. Indeed, if there are multiple retransmission opportunities for a packet, independent interference in each slot improves the chances of having one good slot (i.e., with little interference), with respect to the case where the levels of interference at different slots are correlated. See also the related in-depth discussion in [6].

The paper is organized as follows. Section II discusses related work. Section III develops the system model. Section IV introduces our iterative method and performance metrics. Section V applies our results to LoRa. Section VI concludes.

## II. Related Work

Several papers model LPWAN technologies using stochastic geometry for *spatial* aspects jointly with queueing theory for *temporal* aspects [7], [8], [9], [10], [11]. In contrast to our work, packets are retransmitted until they are successfully received, the nodes perform path-loss inversion so that the average received power is at a fixed, predetermined level, and, finally, the levels of interference at different slots are assumed independent. An iterative method to connect the spatial and temporal aspects is also used in [7] to evaluate the performance of random access schemes. Scheduled access and random access are compared in [8]. Another related analytical framework in [9] addresses nodes capable of energy harvesting. Another thread of work in [10], [11] analyzes the performance of different random access schemes in a cellular IoT system for use in sending preambles that secure a subsequent contention-free data channel; an inductive method is developed to find the statistics of the $m$-th slot from those of the $(m-1)$-th slot.

A link-level performance analysis of LoRa [12] computes SINR thresholds for successful decoding in case of two (but not more) overlapping transmissions. It is shown that packets using different Spreading Factors (SFs) are mostly, but not totally, orthogonal, which has ramifications for nodes far away from the gateway (and is considered in the paper at hand).

Motivated by the specifics of the physical layer of LoRa, several papers analyze its performance assuming that the correct reception depends on the *strongest* interferer's power and not the *cumulative* interference power [13], [14], [15]. As LoRa and other LPWANs evolve toward denser deployments, the number of interferers increases, diminishing the accuracy

of the strongest interferer assumption. For this reason, this work assumes the interference effects to be cumulative.

Finally, [16] analyzes the performance of NB-IoT in a setting with retransmissions. The interdependence of the (re)transmission successes across different slots is modeled using a *reduction factor* but without mathematical justification.

## III. System Model

The system comprises a *gateway*, placed at the origin $o$, and a random number of *nodes* distributed according to a Poisson point process (PPP) $\Phi$ with uniform intensity $\lambda$ on the disk $\mathcal{B} \subseteq \mathbb{R}^2$ centered at $o$ with radius $R$. All nodes create data with the same average rate. The nodes are either static or mobile.[1]

The medium access protocol is Slotted Aloha with a limited number of retransmissions. Time is divided into slots, indexed by $t \in \mathbb{N}$. In each slot, each node transmits a DATA packet to the gateway, with some probability, independently of other nodes. If the gateway receives the packet correctly, it responds with an ACK (acknowledgment), transmitted over a control channel and always received correctly.[2] If the packet is not received correctly, a timeout of random duration occurs and the process is repeated for up to $N$ retransmissions.[3]

The probability that a node transmits a *new* packet in a slot is $p_0 m(\|\mathbf{x}\|)$, where $\mathbf{x} \in \mathcal{B}$ is the node's location and $m(\cdot) \geq 1$ is a function modeling the *modulation and coding schemes (MCSs)* used by nodes. The use of this function enables us to model situations where different nodes select different MCSs (each with its own data rate) depending on their distance from the gateway and, hence, some nodes may have to transmit more often to ensure that all their data participate in the aforementioned (re)transmissions scheme. Selecting different MCSs counters the fact that the received power diminishes with distance, and so some nodes may have to transmit with lower data rates. The normalizing parameter $p_0$ specifies the rate at which new traffic is introduced to the system by each node, and is set to such a value that the minimum value of the MCS function, corresponding to the highest-rate MCS, is 1.

We assume that the locations of DATA packets transmitted *or* retransmitted at each slot also form a PPP with intensity $\lambda p(\|\mathbf{x}\|) m(\|\mathbf{x}\|)$ at location $\mathbf{x}$. The *sending density function* $p(\cdot)$ models transmissions *and* retransmissions, thus

$$p_0 \leq p(\cdot) \leq (N+1) p_0. \tag{1}$$

The lower bound applies if no retransmissions are allowed or all transmissions are successful. The upper bound applies if all (re)transmissions are unsuccessful. Otherwise, $p(\cdot)$ is unknown, and needs to be computed (see Section IV).

All nodes transmit with power $P_t$. All transmissions are susceptible to path loss and Rayleigh fading, so that a packet from location $\mathbf{x}$ arrives at the gateway with power $P_{\mathbf{x}} = P_t \ell(\|\mathbf{x}\|) h_{\mathbf{x}}^2$. The *path loss* $\ell(\cdot)$ models the decay of transmitted power due to distance. In deriving numerical results, we assume $\ell(d) = d^{-\alpha}$, where $\alpha > 2$ is the *decay exponent*. The *fading coefficient* $h_{\mathbf{x}}^2$ models multipath fading. For Rayleigh fading, it is exponentially distributed with mean equal to unity. The fading coefficients at different locations and different slots are independent of each other.

We now describe the model for deciding if a transmission from location $\mathbf{x}$ of a DATA packet is successful. Firstly, let the *signal to interference and noise ratio (SINR)* be:

$$\mathrm{SINR}_{\mathbf{x}} \triangleq \frac{\ell(\|\mathbf{x}\|) h_{\mathbf{x}}^2}{\zeta(\|\mathbf{x}\|) + \sum_{\mathbf{y} \in \Phi_{\mathbf{x}}} d(\|\mathbf{x}\|, \|\mathbf{y}\|) \ell(\|\mathbf{y}\|) h_{\mathbf{y}}^2 \gamma_{\mathbf{y}}}. \tag{2}$$

Here, $\zeta(\|\mathbf{x}\|)$ is the thermal noise power normalized by the transmitter power as a function of the distance $\|\mathbf{x}\|$, e.g., if we use different transmission bandwidths depending on $\|\mathbf{x}\|$. Also, $\Phi_{\mathbf{x}}$ is the PPP of all nodes excluding the node at location $\mathbf{x}$, and $\gamma_{\mathbf{y}}$ is a Bernoulli random variable (RV) which is 1 if the node located at $\mathbf{y}$ interferes with the transmission and 0 if it does not (because, e.g., the node is silent or spread spectrum techniques are used). Regarding the parameters of these Bernoulli RVs, we assume that two simultaneously transmitting nodes (located at distances $d_1$ and $d_2$) interfere with each other with probability $c(d_1, d_2)$. This function can be selected according to the system analyzed. Finally, $d(\|\mathbf{x}\|, \|\mathbf{y}\|)$ is a *damping factor* which can be used to model the near-orthogonality of different SFs of LoRa [12].

Secondly, the transmission is successful iff the SINR exceeds a distance-dependent threshold $\theta(\|\mathbf{x}\|)$, i.e., $\mathrm{SINR}_{\mathbf{x}} \geq \theta(\|\mathbf{x}\|)$. Thus, we consider that different MCSs, used at different distances, require different SINRs for successful reception.

Finally, we assume that the volume of transmitted data per slot from location $\mathbf{x}$ is $v(\|\mathbf{x}\|)$; we do not take it to be constant again due to the potential utilization of multiple MCSs.

## IV. Iterative Computation of Sending Density

### A. Iterative method

We defined the sending density function $p(\cdot)$ but did not show how to calculate it, as the expected number of retransmissions at each location $\|\mathbf{x}\|$ was not specified. We now develop an iterative method to calculate $p(\cdot)$.

Let $\mathcal{S}_n$, $n = 1, 2, \ldots$, be the event that a node transmits packets successfully in $n$ consecutive attempts, not necessarily taking place in consecutive slots. The probability of this event, under the condition that the node is located at $\mathbf{x}$ and at distance $d = \|\mathbf{x}\|$ from the gateway, is given by (3) (cf. Section 3.8.2 of [17], for a simpler, two-slot setting).

In (3), $(a)$ means that the event $\mathcal{S}_n$ is equivalent to the event that all $\mathrm{SIR}_{\mathbf{x}}(i)$, $i = 1, \ldots, n$, during the $n$ slots, exceed the threshold $\theta(d)$. In $(b)$, we write the expectation of the probability with respect to all RVs except the $n$ fading coefficients $h_{\mathbf{x}}^2(i)$, $i = 1, \ldots, n$, and then use the pdf of the exponential RV $h_{\mathbf{x}}^2(i)$. In $(c)$, we use the law of nested expectation and a rearrangement of terms. In $(d)$, we calculate the inner expectations first w.r.t. the fading coefficients of

[1] Mobile nodes move at a speed that does not allow the topology to change noticeably while a node attempts to send a packet to the gateway. This approach is justified as we focus on WANs with large communication ranges.

[2] An alternative model is that ACKs are also susceptible to interference.

[3] Our analysis can be applied with minor changes to the case where *preambles* rather than packets compete for channel access. Successful packet transmission is guaranteed here as soon as the channel is "cleared" by the successful transmission of a preamble.

$$
\begin{aligned}
&\mathbb{P}[\mathcal{S}_n|d] \overset{(a)}{=} \mathbb{P}[\mathrm{SIR}_{\mathbf{x}}(1) \geq \theta(d), \ldots, \mathrm{SIR}_{\mathbf{x}}(n) \geq \theta(d)] \\
&= \mathbb{P}\left[ \frac{\ell(d) h_{\mathbf{x}}^2(1)}{\zeta(d) + \sum\limits_{y \in \Phi_{\mathbf{x}}} d(\|\mathbf{x}\|, \|\mathbf{y}\|) \ell(\|\mathbf{y}\|) h_{\mathbf{y}}^2(1) \gamma_{\mathbf{y}}(1)} \geq \theta(d), \ldots, \frac{\ell(d) h_{\mathbf{x}}^2(n)}{\zeta(d) + \sum\limits_{y \in \Phi_{\mathbf{x}}} d(\|\mathbf{x}\|, \|\mathbf{y}\|) \ell(\|\mathbf{y}\|) h_{\mathbf{y}}^2(n) \gamma_{\mathbf{y}}(n)} \geq \theta(d) \right] \\
&\overset{(b)}{=} \mathbb{E}\left[ \prod_{i=1}^{n} \exp\left( - \frac{\theta(d) \left( \zeta(d) + \sum\limits_{\mathbf{y} \in \Phi_{\mathbf{x}}} d(\|\mathbf{x}\|, \|\mathbf{y}\|) \ell(\|\mathbf{y}\|) h_{\mathbf{y}}^2(i) \gamma_{\mathbf{y}}(i) \right)}{\ell(d)} \right) \right] \\
&\overset{(c)}{=} \exp\left[ \frac{-n\theta(d)\zeta(d)}{\ell(d)} \right] \mathbb{E}_{\Phi}\left[ \prod_{\mathbf{y} \in \Phi_{\mathbf{x}}} \prod_{i=1}^{n} \mathbb{E}_{h,\gamma}\left[ \exp\left( - \frac{\theta(d) d(\|\mathbf{x}\|, \|\mathbf{y}\|) \ell(\|\mathbf{y}\|) h_{\mathbf{y}}^2(i) \gamma_{\mathbf{y}}(i)}{\ell(d)} \right) \right] \right] \\
&\overset{(d)}{=} \exp\left[ \frac{-n\theta(d)\zeta(d)}{\ell(d)} \right] \mathbb{E}_{\Phi}\left[ \prod_{\mathbf{y} \in \Phi_{\mathbf{x}}} \left( 1 - p(\|\mathbf{y}\|) m(\|\mathbf{y}\|) c(d, \|\mathbf{y}\|) + \frac{p(\|\mathbf{y}\|) m(\|\mathbf{y}\|) c(d, \|\mathbf{y}\|)}{1 + \theta(d) d(\|\mathbf{x}\|, \|\mathbf{y}\|) \ell(\|\mathbf{y}\|)/\ell(d)} \right)^n \right] \\
&\overset{(e)}{=} \exp\left[ \frac{-n\theta(d)\zeta(d)}{\ell(d)} \right] \exp\left[ -\lambda \int_{\mathcal{B}} \left( 1 - \left( 1 - p(\|\mathbf{y}\|) m(\|\mathbf{y}\|) c(d, \|\mathbf{y}\|) + \frac{p(\|\mathbf{y}\|) m(\|\mathbf{y}\|) c(d, \|\mathbf{y}\|)}{1 + \theta(d) d(\|\mathbf{x}\|, \|\mathbf{y}\|) \ell(\|\mathbf{y}\|)/\ell(d)} \right)^n \right) \mathrm{d}y \right]. \quad (3)
\end{aligned}
$$

the interferers (using the moment generating function of the exponential RV) and then the Bernoulli RVs. Finally, in $(e)$, we apply the probability generating functional of the PPP [17].

Next, let $\mathcal{F}_n$ be the event that a node fails to transmit the packet in $n$ consecutive attempts, not necessarily in consecutive slots. Let $\mathcal{A}_i$, $i = 1, \ldots, n$ be the event that the $i$-th attempt is a success. The probability of $\mathcal{F}_n$ for a node at a distance $d$ is ($(a)$ uses the inclusion-exclusion principle):

$$
\begin{aligned}
\mathbb{P}(\mathcal{F}_n|d) &= \mathbb{P}(\mathcal{A}_1' \cap \cdots \cap \mathcal{A}_n'|d) = 1 - \mathbb{P}(\mathcal{A}_1 \cup \cdots \cup \mathcal{A}_n|d) \\
&\overset{(a)}{=} 1 - \sum_i \mathbb{P}(\mathcal{A}_i|d) + \sum_{1 \leq i < j \leq n} \mathbb{P}(\mathcal{A}_i \cap \mathcal{A}_j|d) \\
&\quad - \cdots + (-1)^n \mathbb{P}(\mathcal{A}_1 \cap \cdots \cap \mathcal{A}_n|d) \\
&= \sum_{i=0}^{n} \binom{n}{i} (-1)^i \mathbb{P}(\mathcal{S}_i|d), \quad (4)
\end{aligned}
$$

where we set $\mathbb{P}(\mathcal{S}_0|d) = 1$. As $\mathbb{E}(X) = \sum_{n=1}^{\infty} \mathbb{P}(X \geq n)$ for any RV $X$ taking nonnegative integer values, the expected number of retransmissions per packet for a node at distance $d$ is $\sum_{n=1}^{N} \mathbb{P}(\mathcal{F}_n|d)$. Adding the original transmission, the sending density function is:

$$
p(d) = p_0 \left[ 1 + \sum_{n=1}^{N} \mathbb{P}(\mathcal{F}_n|d) \right]. \quad (5)
$$

It uses the probabilities $\mathbb{P}(\mathcal{F}_n|d)$ from (4), which are in turn computed using $\mathbb{P}(\mathcal{S}_n|d)$ from (3), which are calculated using $p(d)$, closing the cycle. Thus, (3), (4), and (5) suggest an iterative method for finding $p(d)$: We set $p(d)$ equal to an arbitrary function $p^0(d)$, run $p^0(d)$ through (3), (4), and (5) to compute an updated function $p^1(d)$, and repeat the process a few times until effective convergence to a limit function $p^\infty(d)$, at which point we set $p(d)$ equal to that limit.

The iteration specified by (3), (4), and (5) is complicated. Thus, a formal proof of convergence (using, e.g., a fixed point theorem) is beyond the scope of this paper. However, we have always observed convergence in practice and also validated by simulation the limit the iteration arrives at, as discussed next.

### *B. Numerical evaluations*

Fig. 1a shows the convergence of the proposed method. Black lines show the first few iterations starting from the lower bound $p^0(d) = p_0$; red lines show the first few iterations starting from the upper bound $p^0(d) = p_0(N+1)$. In both cases, the curves approach the same limit, which is an indication for convergence. We tried other starting functions as well, such as piecewise constant ones that satisfy (1), and observed that they all invariably arrive at the same limiting function.

Fig. 1b plots the normalized sending density $p(d)/p_0$ for different values of $p_0$, as arrived at using the iterative method. The normalization is required to allow for a simple joint plot. All values are naturally lower bounded by 1 (for no retransmissions) and upper bounded by 3 (when each packet is retransmitted for the maximum of $N + 1 = 3$ times). With higher $p_0$, even nodes close to the gateway have to retransmit as often as possible, whereas for low $p_0$, only a few retransmissions are needed over the whole range. In the same figure, and especially for the values $p_0 = 0.0001$ and $p_0 = 0.001$, we superimpose on each of the respective plots a scatterplot created by simulation experiments. In each experiment, we create and simulate a single network realization and for each node of that realization we plot a point whose $x$-coordinate is the distance of the node from the gateway and $y$-coordinate is the average number of (re)transmissions per data packet. Observe that the scatterplot matches well $p(d)/p_0$ which, by (5), is the average number of (re)transmissions predicted by the model. In our simulations, after a failure each node

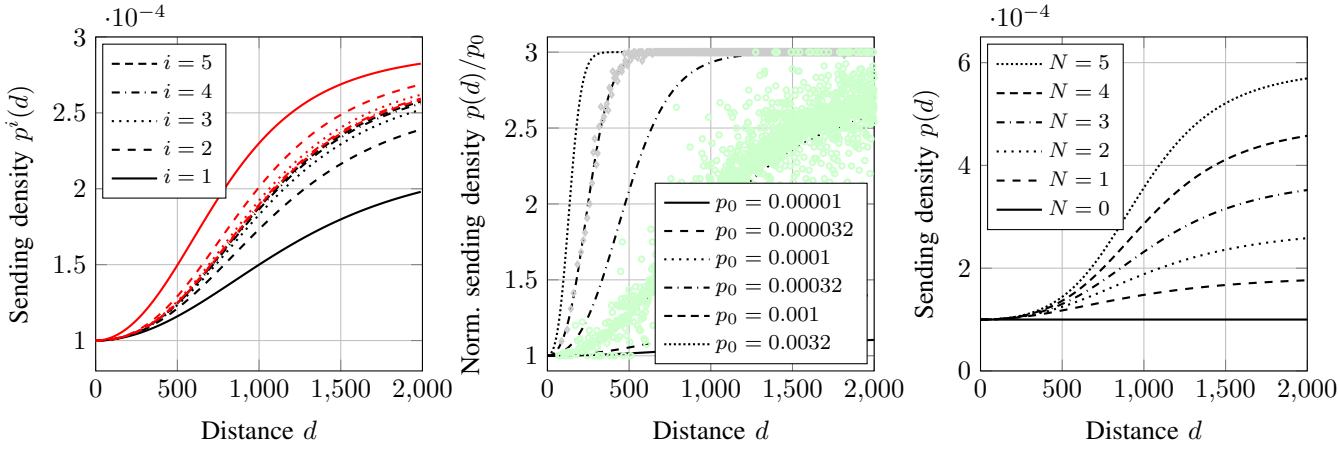


(a) Sending density sequence $p^i(d)$ over 5 iterations. Black curves show results when starting with $p^0(d) \equiv p_0$; red curves show results when starting with $p^0(d) \equiv p_0 N$.

(b) Normalized sending density $p(d)/p$ for different values of $p_0$ after 8 iterations. Lines are theoretical results and marks are simulations for two selected values of $p_0$.

(c) Sending density $p(d)$ for different values of $N$.

Fig. 1: Sending density as a function of the distance $d$. Parameters (unless specified otherwise): $\alpha = 3$, $\lambda = 0.001$, $R = 2000$, $p_0 = 0.0001$, $N = 2$, $\theta(d) = 1$, $c(\cdot,\cdot) = 1$, $\zeta(\cdot) = 0$, $d(\cdot,\cdot) = 1$, and $m(\cdot) = 1$.

retransmits immediately in the next slot, rather than waiting for a random time, as assumed in our model. As a consequence, the simulated average number of (re)transmissions is slightly larger than the average number computed with the iterative process from (5).

Finally, Fig. 1c studies the impact of $N$: As $N$ increases, it is mainly the distant nodes that make use of retransmissions; however, the eventual convergence of $p(d)$ to its maximum value suggests that these retransmissions are of little use.

### C. Performance metrics

Important performance metrics can be derived from $p(\cdot)$ and hence can also be computed once the iterative method is applied.

The *outage probability* $\mathbb{P}_{\text{out}}(d) = \mathbb{P}[\mathcal{F}_{N+1}|d]$ is the probability that a packet originating at a distance $d$ from the gateway will not be successfully received in any of the $N+1$ (re)transmissions. The *throughput density* $T(d)$ is defined such that $T(d)\,\mathrm{d}r$ is the incremental volume of data per slot that nodes within the ring centered at $o$ with inner and outer radii $d$ and $d + \mathrm{d}r$ transmit successfully. With packet size $v(d)$, we have $T(d) = 2\pi d\,\lambda\,p_0\,m(d)\,v(d)\,[1 - \mathbb{P}_{\text{out}}(d)]$. The *average throughput* $\overline{T}$ is the average volume of successfully received data during a slot: $\overline{T} = \int_o^R T(r)\,\mathrm{d}r$. The *energy consumption* $E(d)$ is the average energy consumed for the successful transmission of a single bit at distance $d$. We make the normalizing assumption that the transmission during a single slot results to a dissipation of energy equal to unity, and note that the average number of transmissions (including the initial transmission) per packet is $p(d)/p_0$. Thus, to transmit $v(d)$ bits with probability $1 - \mathbb{P}_{\text{out}}(d)$ requires $p(d)/p_0$ units of energy, so it follows that

$$E(d) = \frac{p(d)}{p_0 v(d)(1 - \mathbb{P}_{\text{out}}(d))}.$$

## V. Performance Evaluation of a LoRa Model

### A. LoRa model

LoRa offers a favorable mix of reliability, long-range communication, and low power consumption. This makes it a promising choice in a variety of settings, ranging from industrial IoT [1] to vehicular networks [18]. However, to ensure good performance, key parameters have to be fine-tuned properly; one of these is the maximum number $N$ of retransmissions for lost packets. In the following, we plot the above performance metrics, for the case of LoRa, with the goal of exploring their tradeoffs and providing guidelines for selecting an optimal $N$ for a given scenario.

The physical layer of LoRa has some particularities [12], [19], [20] that must be captured by our model. Firstly, LoRa makes use of six SFs, SF7 to SF12, depending on the distance. Increasing the SF by one roughly doubles the symbol duration and decreases the SINR threshold $\theta(\|\mathbf{x}\|)$. We apply SF7 for $d < 250$, SF8 for $250 \le d < 500$, etc., until SF12 for $d \ge 1250$. For our model, this implies that $m(\|\mathbf{y}\|) = 2^{(i-7)}$ for SF$i$. The threshold $\theta(\|\mathbf{x}\|)$ is assigned depending on the SF$i$, by choosing a value $(-6, -9, -12, -15, -17.5, -20)$ dB for SF7 to SF12, respectively. For transmissions using SF$i$, interferers that apply a SF$j$ with $j \neq i$ interfere weakly with the transmission as compared to interferers with SF$i$. Hence, an inter-SF damping factor $d(\|\mathbf{x}\|, \|\mathbf{y}\|)$ is used, which takes values in dB from the matrix

$$d_{(i,j)} = \begin{pmatrix} 0 & -8 & -9 & -9 & -9 & -9 \\ -11 & 0 & -11 & -12 & -13 & -13 \\ -15 & -13 & 0 & -13 & -14 & -15 \\ -19 & -18 & -17 & 0 & -17 & -18 \\ -22 & -22 & -21 & -20 & 0 & -20 \\ -25 & -25 & -25 & -24 & -23 & 0 \end{pmatrix}, \quad (6)$$

where $i$ and $j$ indicate the SF of the transmitter and interferer.

Unless otherwise specified, we apply our iterative method for 5 iterations and set $N = 3$, $\alpha = 3$, $\lambda = 0.001$, $R = 2000$, $p_0 = 0.001$, $v(d) = 200/2^{i-7}$, $c(\cdot,\cdot) = 1$, and $\zeta(\cdot) = 0$.

### B. Performance evaluation

Fig. 2 shows the outage probability of a LoRa node located at distance $d$ from the gateway versus the maximum number of retransmissions $N$. Observe that a higher number of retransmissions helps nodes at small distances, but the curves swap order at around $d = 1000$ where more retransmissions start to increase outage due to interference. The intersection point depends on the system parameters: if, e.g., the traffic is increased (larger $p_0$) or the node density increases (higher $\lambda$), the intersection moves to smaller distances (not shown).

The blue symbols show the outage probability determined by the LoRaSim simulator [21], which we enhanced to incorporate fading on the links as well as ACKs and retransmissions. There is a good match between theory and simulation; we attribute the discrepancy for low outage probabilities on the fact that the relative error in estimating the outage probability becomes larger as this probability decreases and, hence, fewer outage events are measured in the simulations.

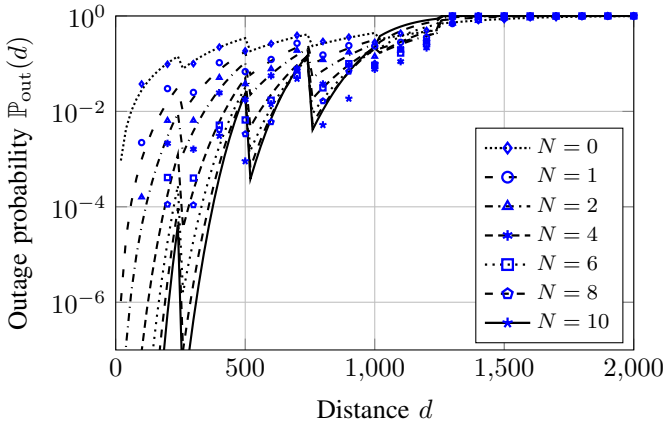


Fig. 2: Outage probability $\mathbb{P}_{\text{out}}(d)$ versus distance $d$ and maximum number of retransmissions $N$. Lines present theory; marks present simulation results.

Fig. 3 shows the energy consumption $E(d)$ of a successfully transmitted bit. It increases with distance, as outage increases with distance, in turn both increasing the number of retransmissions (up to the maximum) and reducing the average number of successfully transmitted bits per transmission. However, there are also sudden jumps in the average energy consumption when the SF increases, raising the question of optimizing the distances allocated to each SF with respect to this metric and not only the throughput density (cf. Figs. 5a and 5b.)

Fig. 4 shows the throughput $\bar{T}$ versus $p_0$ and $N$. For all values of $p_0$, there is an optimal $N$, and the corresponding optimal value of $\bar{T}$ strongly depends on $p_0$. For smaller values of $p_0$, this optimum is in the range of one to five (black curves). For higher values of $p_0$, this optimum is more pronounced than for lower values. If $p_0 > 0.001$, interference becomes high and

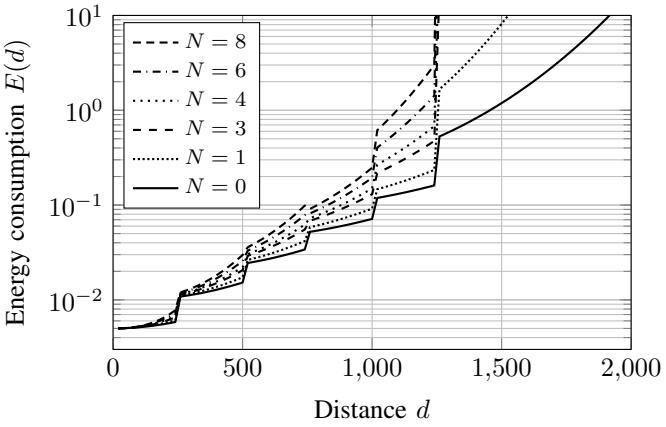


Fig. 3: Energy consumption $E(d)$ for LoRa versus distance $d$ and maximum number of retransmissions $N$.

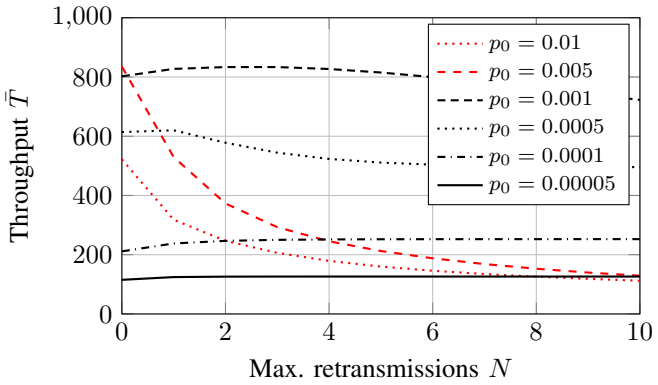


Fig. 4: Throughput $\bar{T}$ for LoRa versus $p_0$ and the maximum number of retransmissions $N$.

thus any additional interference from retransmissions reduces the throughput (red curves), making $N = 0$ the best choice.

Fig. 5a shows the throughput density $T(d)$ versus the distance $d$ and $p_0$ for $N = 3$. The plot has three regimes: In the low $p_0$-regime, the throughput density increases linearly with $d$, which implies a fair performance at all distances, as the number of nodes in a ring of width d$r$ also increases linearly with $d$. In the medium $p_0$-regime, the throughput density increases up to a point beyond $d = 1000$ and then sharply falls off. Finally, in the high $p_0$-regime, only nodes near the gateway get a meaningful throughput density, whereas all others almost cannot reach the gateway at all. This effectively reduces the network size, rendering distant nodes merely sources of interference that do not contribute to the overall throughput. Hence, in such a scenario, it would be better for them to switch off. Finally, observe that using multiple SFs helps nodes that are farther from the gateway, but to a limited degree.

Finally, Fig. 5b shows throughput density again, but this time for different values of $N$ and a mid-range sending probability of $p_0 = 0.001$. Note that retransmissions mostly benefit nodes at medium distances, roughly between 300 and 1000. For closer nodes, additional retransmissions do not

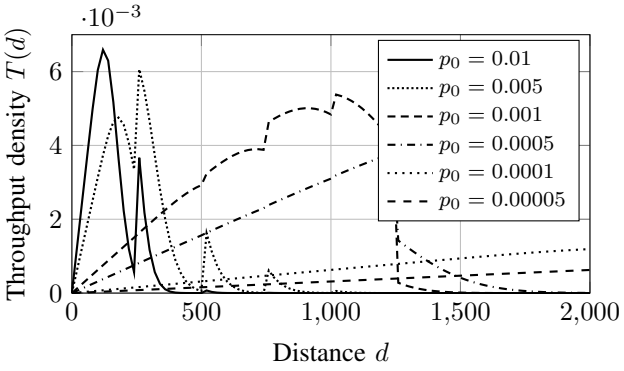


(a) $T(d)$ versus $d$ and $p_0$ for $N = 3$.

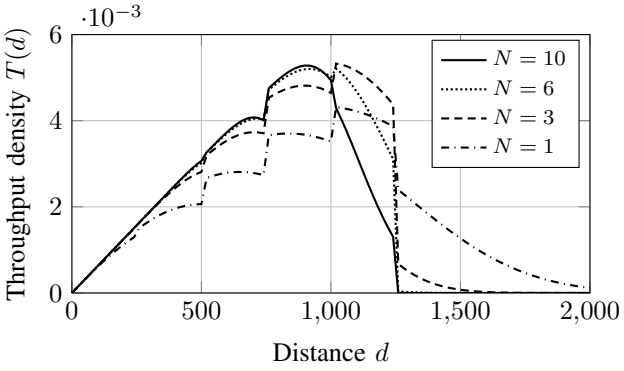


(b) $T(d)$ versus $d$ and $N$ for $p_0 = 0.001$.

Fig. 5: Throughput density $T(d)$ for LoRa versus the distance $d$, the maximum number of retransmissions $N$, and $p_0$.

improve the performance a lot, as they are almost not required. For more distant nodes, these retransmissions cause too much interference and notably degrade their already weak performance in the given scenario. Finally, similar to Fig. 3, using multiple SFs leads to modest improvement for distant nodes.

## VI. Conclusions

Using a simple model for an LPWAN cell that employs slotted Aloha with a limited number of retransmissions in the uplink, we propose an iterative method to calculate the traffic density, facilitating the derivation of several performance metrics.

Applying the model in LoRa yields useful insights for the efficient use of this technology. Notably, *(i)* the increasing SF mechanism helps in permitting larger-sized cells albeit with increased energy consumption (Figs. 2, 3), *(ii)* larger values of $p_0$ (i.e., the intensity with which new packets arrive) diminish the cell's effective radius (Fig. 5a), *(iii)* the optimal number of retransmissions strongly depends on $p_0$ (Fig. 4) and *(iv)* more retransmissions decrease the outage probability of nodes closer to the gateway but hurt those farther away (Figs. 2, 5).

## Acknowledgments

This work was supported by the Austrian Klima und Energiefonds under grant 881161 (ConSens) of the Austrian Research Promotion Agency (FFG); the Austrian Science Fund (FWF) under grant P24480-N15; the Hellenic Foundation for Research and Innovation under project HFRI-FM17-352 (Acronym: LEMONADE); and the Science and Engineering Research Board (SERB), Government of India, under grant SRG/2020/001491. The tools DeepL, Grammarly, and ChatGPT were used to obtain suggestions for improving language and grammar.

## References

[1] M. Jouhari, N. Saeed, M.-S. Alouini, and E. M. Amhoud, "A survey on scalable LoRaWAN for massive IoT: Recent advances, potentials, and challenges," *IEEE Commun. Surveys & Tutorials*, 2023.

[2] J. de Carvalho Silva, J. J. Rodrigues, A. M. Alberti, P. Solic, and A. L. Aquino, "LoRaWAN—a low power WAN protocol for Internet of Things: A review and opportunities," in *SpliTech*, 2017, pp. 1–6.

[3] A. Lavric, A. I. Petrariu, and V. Popa, "Long range SigFox communication protocol scalability analysis under large-scale, high-density conditions," *IEEE Access*, vol. 7, pp. 35 816–35 825, 2019.

[4] C. B. Mwakwata, H. Malik, M. Mahtab Alam, Y. Le Moullec, S. Parand, and S. Mumtaz, "Narrowband internet of things (NB-IoT): From physical (PHY) and media access control (MAC) layers perspectives," *Sensors*, vol. 19, no. 11, p. 2613, 2019.

[5] Q. Hamarsheh, O. Daoud, M. Baniyounis, and A. Damati, "Narrowband internet-of-things to enhance the vehicular communications performance," *Future Internet*, vol. 15, no. 1, p. 16, 2022.

[6] R. Vaze, "Throughput-delay-reliability tradeoff with ARQ in wireless ad hoc networks," *IEEE Trans. Wireless Commun.*, vol. 10, no. 7, pp. 2142–2149, 2011.

[7] M. Gharbieh, H. ElSawy, A. Bader, and M.-S. Alouini, "Spatiotemporal stochastic modeling of IoT enabled cellular networks: Scalability and stability analysis," *IEEE Trans. Commun.*, pp. 3585–3600, 2017.

[8] M. Gharbieh, H. ElSawy, H.-C. Yang, A. Bader, and M.-S. Alouini, "Spatiotemporal model for uplink IoT traffic: Scheduling and random access paradox," *IEEE Trans. Wireless Commun.*, pp. 8357–8372, 2018.

[9] M. Gharbieh, H. ElSawy, M. Emara, H.-C. Yang, and M.-S. Alouini, "Grant-free opportunistic uplink transmission in wireless-powered IoT: A spatio-temporal model," *IEEE Trans. Commun.*, vol. 69, no. 2, pp. 991–1006, 2020.

[10] N. Jiang, Y. Deng, X. Kang, and A. Nallanathan, "Random access analysis for massive IoT networks under a new spatio-temporal model: A stochastic geometry approach," *IEEE Trans. Commun.*, vol. 66, no. 11, pp. 5788–5803, 2018.

[11] N. Jiang, Y. Deng, A. Nallanathan, X. Kang, and T. Q. Quek, "Analyzing random access collisions in massive IoT networks," *IEEE Trans. Wireless Commun.*, vol. 17, no. 10, pp. 6853–6870, 2018.

[12] D. Croce, M. Gucciardo, S. Mangione, G. Santaromita, and I. Tinnirello, "Impact of LoRa imperfect orthogonality: Analysis of link-level performance," *IEEE Commun. Letters*, vol. 22, no. 4, pp. 796–799, 2018.

[13] O. Georgiou and U. Raza, "Low power wide area network analysis: Can LoRa scale?" *IEEE Wireless Commun. Letters*, pp. 162–165, 2017.

[14] L. Beltramelli, A. Mahmood, P. Österberg, and M. Gidlund, "LoRa beyond ALOHA: An investigation of alternative random access protocols," *IEEE Trans. Industrial Informatics*, vol. 17, no. 5, pp. 3544–3554, 2020.

[15] S. S. Borkotoky, J. F. Schmidt, U. Schilcher, P. Battula, and S. Rathi, "Reliability and energy consumption of LoRa with bidirectional traffic," *IEEE Commun. Letters*, vol. 25, no. 11, pp. 3743–3747, 2021.

[16] J. Xing, W. Xue-Dong, W. Xiao-Wei, P. Dan, L. Cai-Hua, and L. Long-Ya, "Performance analysis of narrow-band IoT coverage enhancement based on repetition and retransmission," in *IEEE ICCC*, 2020.

[17] M. Haenggi and R. K. Ganti, "Interference in large wireless networks," *Foundations and Trends in Networking*, vol. 3, no. 2, 2009.

[18] F. M. Ortiz, T. T. de Almeida, A. E. Ferreira, and L. H. M. Costa, "Experimental vs. simulation analysis of LoRa for vehicular communications," *Computer Communications*, vol. 160, pp. 299–310, 2020.

[19] L. Beltramelli, A. Mahmood, M. Gidlund, P. Österberg, and U. Jennehag, "Interference modelling in a multi-cell LoRa system," in *WiMob*, 2018.

[20] S. S. Borkotoky, U. Schilcher, and C. Bettstetter, "Cooperative relaying in LoRa sensor networks," in *IEEE GLOBECOM*, 2019.

[21] LoRaSim webpage, https://mcbor.github.io/lorasim/, Access date: June 2, 2023.